


AUTHOR QUERY FORM

 ELSEVIER	Journal: Nonlinear Analysis: Real World Applications Article Number: 2301	Please e-mail your responses and any corrections to: E-mail: corrections.esch@elsevier.river-valley.com
--	--	--

Dear Author,

Please check your proof carefully and mark all corrections at the appropriate place in the proof (e.g., by using on-screen annotation in the PDF file) or compile them in a separate list. Note: if you opt to annotate the file with software other than Adobe Reader then please also highlight the appropriate place in the PDF file. To ensure fast publication of your paper please return your corrections within 48 hours.

For correction or revision of any artwork, please consult <http://www.elsevier.com/artworkinstructions>.

Your article is registered as a regular item and is being processed for inclusion in a regular issue of the journal. If this is NOT correct and your article belongs to a Special Issue/Collection please contact n.sunder@elsevier.com immediately prior to returning your corrections.

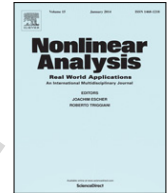
Location in article	Query/Remark click on the Q link to go Please insert your reply or correction at the corresponding line in the proof
Q1	Please confirm that given names and surnames have been identified correctly.
Q2	Color statement has been added to the caption(s) of Figs. 2 and 3. Please check, and correct if necessary.
Q3	Both color and monochrome figures are present in the source file and processed as separately for print and web versions. Please check, and correct if necessary.
	<div style="border: 1px solid black; padding: 5px; display: inline-block;"> <p style="color: red; margin: 0;">Please check this box or indicate your approval if you have no corrections to make to the PDF file</p> <input style="width: 30px; height: 20px; vertical-align: middle;" type="checkbox"/> </div>

Thank you for your assistance.



Contents lists available at ScienceDirect

Nonlinear Analysis: Real World Applications

www.elsevier.com/locate/nonrwa


Chaotic dynamics in three dimensions: A topological proof for a triopoly game model

Q1 Marina Pireddu*

[^]
 Department of Mathematics and Applications, University of Milano-Bicocca, Milano, Italy


ARTICLE INFO

Article history:

Received 15 May 2013

Accepted 10 March 2015

Available online xxxx

Keywords:

Chaotic dynamics

Stretching along the paths

Triopoly games

Heterogeneous players

ABSTRACT

We rigorously prove the existence of chaotic dynamics for a triopoly game model. In the model considered, the three firms are heterogeneous and in fact each of them adopts a different decisional mechanism (i.e., linear approximation, best response and gradient mechanisms, respectively).

The method we employ is the so-called “Stretching Along the Paths” (SAP) technique, based on the Poincaré–Miranda Theorem and on the properties of the cutting surfaces.

© 2015 Published by Elsevier Ltd.

1. Introduction

In the economic literature, due to the complexity of the models considered, an analytical study of the associated dynamical features turns out often to be too difficult or simply impossible to perform. That is why many dynamical systems are studied mainly from a numerical viewpoint (see, for instance, [1–4]). Sometimes, however, even such kind of study turns out to be problematic, especially with high-dimensional systems, where several variables are involved [5].

In particular, as observed in Naimzada and Tramontana’s working paper [6], this may be the reason for the relatively low number of works on triopoly games (see, for instance, [7–9]), where the context is given by an oligopoly composed by three firms. In such framework, a local analysis can generally be performed in the special case of homogeneous triopoly models, i.e., those in which the equations describing the dynamics are symmetric (see, for instance, [10–12]).

A more difficult task is that of studying heterogeneous triopolies, where the three firms considered behave according to different strategies. In fact, in the absence of complete information, both in regard to the shape of the demand function and with respect to the competitors’ future output choices, in those models it is

* Correspondence to: University of Milano-Bicocca, U5 Building, Via Cozzi 53, 20125 Milano, Italy. Tel.: +39 0264485729; fax: +39 0264485705.

E-mail address: marina.pireddu@unimib.it.

assumed that at each time period firms decide how much to produce in the following period according to different behavioral mechanisms. See [13–15] for some works on oligopolies with boundedly rational players, while the study of heterogeneous triopolies has been performed, for instance, in [16,17], as well as in the above mentioned paper by Naimzada and Tramontana [6]. In this latter work, in addition to the classical heterogeneity with interacting agents adopting gradient and best response mechanisms, it is assumed that one of the firms adopts a linear approximation mechanism, which means that the firm does not know the shape of the demand function and thus builds a conjectured demand function through the local knowledge of the true demand function. In regard to such model, those authors perform a stability analysis of the Nash equilibrium and show numerically that, according to the choice of the parameter values, it undergoes a flip bifurcation or a Neimark–Sacker bifurcation leading to chaos.

What we then aim to do in the present paper is complementing that analysis, by proving the existence of chaotic sets for the model in [6] only via topological arguments. This task will be performed using the “Stretching Along the Paths” (from now on, SAP) technique, already employed in [18] to rigorously prove the presence of chaos for some discrete-time one- and bi-dimensional economic models of the classes of overlapping generations and duopoly game models. Notice however that, to the best of our knowledge, this is the first three-dimensional discrete-time application of the SAP technique, called in this way because it concerns maps that expand the arcs along one direction and are instead compressive in the remaining directions. We stress that, differently from other methods for the search of fixed points and the detection of chaotic dynamics based on more sophisticated algebraic or geometric tools, such as the Conley index or the Lefschetz number (see, for instance, [19–21]), the SAP method relies on relatively elementary arguments and it is easy to apply in practical contexts, without the need of ad-hoc constructions. No differentiability conditions are required for the map describing the dynamical system under analysis and even continuity is needed only on particular subsets of its domain. Moreover, the SAP technique can be used to rigorously prove the presence of chaos also for continuous-time dynamical systems. In fact, in such framework it suffices to apply the results in Section 2, suitably modified, to the Poincaré map associated to the considered system¹ and thus one is led back to work with a discrete-time dynamical system. However, the geometry required to apply the SAP method turns out to be quite different in the two contexts: in the case of discrete-time dynamical systems we look for “topological horseshoes” (see, for instance, [24–26]), that is, a weaker version of the celebrated Smale horseshoe in [27], while in the case of continuous-time dynamical systems one has to consider the case of switching systems and the needed geometry is usually that of the so-called “Linked Twist Maps” (LTMs) (see [28–30]), as shown for the planar case in [22,23]. We also stress that the Poincaré map is a homeomorphism onto its image, while in the discrete-time framework the function describing the considered dynamical system need not be one-to-one, like in our example in Section 3. Hence, in the latter context, it is in general not possible to apply the results for the Smale horseshoe, where one deals with homeomorphisms or diffeomorphisms. As regards three-dimensional continuous-time applications of the SAP method, those have recently been performed in [31], in a higher-dimensional counterpart of the LTMs framework, and in [32], where a system switching between different regimes is considered.

For the reader’s convenience, we are going to recall in Section 2 what are the basic mathematical ingredients behind the SAP method, as well as the main conclusions it allows to draw about the chaotic features of the model under analysis. It will then be shown in Section 3 how it can be applied to the triopoly game model taken from [6]. Some further considerations and comments can be found in Section 4, which concludes the paper.

¹ We stress that, in order to apply the SAP method to continuous-time systems, as done in [22,23], it is not required to know the analytic formulation of the corresponding Poincaré map, but in general it suffices to know the geometry of the orbits in the phase-plane.

2. The “stretching along the paths” method

In this section we briefly recall what the “Stretching along the paths” (SAP) technique consists in, referring the reader interested in further mathematical details to [33], where the original planar theory by Papini and Zanolin in [34,35] has been extended to the N -dimensional setting, with $N \geq 2$.

In the bi-dimensional setting, elementary theorems from plane topology suffice, while in the higher-dimensional framework some results from degree theory are needed, leading to the study of the so-called “cutting surfaces”. In fact, the proofs of the main results in [33] (and in particular of Theorem 2.1), we do not recall here, are based on the properties of the cutting surfaces and on the Poincaré–Miranda Theorem, that is, an N -dimensional version of the Intermediate Value Theorem.

Since in Section 3 we will deal with the three-dimensional setting only, we directly present the theoretical results in the special case in which $N = 3$.

We start with some basic definitions.

A *path* in a metric space X is a continuous map $\gamma : [t_0, t_1] \rightarrow X$. We also set $\bar{\gamma} := \gamma([t_0, t_1])$. Without loss of generality, we usually take the unit interval $[0, 1]$ as the domain of γ . A *sub-path* σ of γ is the restriction of γ to a compact sub-interval of its domain. By a *generalized parallelepiped* we mean a set $\mathcal{P} \subseteq X$ which is homeomorphic to the unit cube $I^3 := [0, 1]^3$, through a homeomorphism $h : \mathbb{R}^3 \supseteq I^3 \rightarrow \mathcal{P} \subseteq X$. We also set

$$\mathcal{P}_\ell^- := h([x_3 = 0]), \quad \mathcal{P}_r^- := h([x_3 = 1])$$

and call them the *left* and the *right* faces of \mathcal{P} , respectively, where²

$$[x_3 = 0] := \{(x_1, x_2, x_3) \in I^3 : x_3 = 0\} \quad \text{and} \quad [x_3 = 1] := \{(x_1, x_2, x_3) \in I^3 : x_3 = 1\}.$$

Setting

$$\mathcal{P}^- := \mathcal{P}_\ell^- \cup \mathcal{P}_r^-,$$

we call the pair

$$\tilde{\mathcal{P}} := (\mathcal{P}, \mathcal{P}^-)$$

an *oriented parallelepiped* of X .

Although in the application discussed in the present paper the space X is simply \mathbb{R}^3 and the generalized parallelepipeds are standard parallelepipeds, so that the similarity with the classical Smale horseshoe is even more apparent (see Figs. 2 and 3), the generality of our definitions makes them applicable in different contexts (see Fig. 1).

We are now ready to introduce the *stretching along the paths* property for maps between oriented parallelepipeds.

Definition 2.1 (SAP). Let $\tilde{\mathcal{A}} := (\mathcal{A}, \mathcal{A}^-)$ and $\tilde{\mathcal{B}} := (\mathcal{B}, \mathcal{B}^-)$ be oriented parallelepipeds of a metric space X . Let also $\psi : \mathcal{A} \rightarrow \mathcal{B}$ be a function and $\mathcal{K} \subseteq \mathcal{A}$ be a compact set. We say that (\mathcal{K}, ψ) *stretches* $\tilde{\mathcal{A}}$ to $\tilde{\mathcal{B}}$ *along the paths*, and write

$$(\mathcal{K}, \psi) : \tilde{\mathcal{A}} \rightarrow \tilde{\mathcal{B}},$$

² Notice that the choice of privileging the third coordinate is purely conventional. In fact, any other choice would give the same results, as it is possible to compose the homeomorphism h with a suitable permutation on three elements, without modifying its image set.

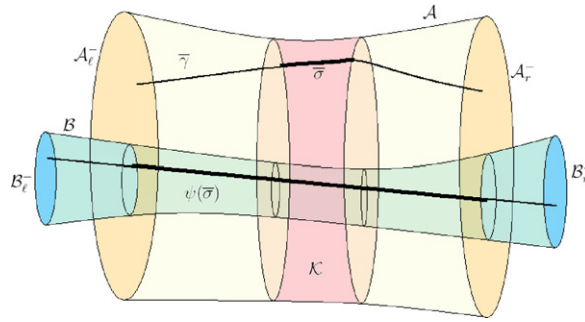


Fig. 1. The tubular sets \mathcal{A} and \mathcal{B} in the picture are two generalized parallelepipeds, for which we have put in evidence the compact set \mathcal{K} and the boundary sets \mathcal{A}_ℓ^- and \mathcal{A}_r^- , as well as \mathcal{B}_ℓ^- and \mathcal{B}_r^- . Since $\psi(\mathcal{A}) = \mathcal{B}$, $\psi(\mathcal{A}_\ell^-) = \mathcal{B}_\ell^-$ and $\psi(\mathcal{A}_r^-) = \mathcal{B}_r^-$, it holds that $(\mathcal{A}, \psi) : \tilde{\mathcal{A}} \rightleftarrows \tilde{\mathcal{B}}$. On the other hand, given the (generic) path γ joining in \mathcal{A} the sides \mathcal{A}_ℓ^- and \mathcal{A}_r^- , the ψ -image of its sub-path σ in \mathcal{K} joins again \mathcal{A}_ℓ^- and \mathcal{A}_r^- in \mathcal{A} and thus we also have that $(\mathcal{K}, \psi) : \tilde{\mathcal{A}} \rightleftarrows \tilde{\mathcal{A}}$. The existence of a fixed point for ψ in \mathcal{K} is then ensured by [Theorem 2.1](#).

if the following conditions hold:

- ψ is continuous on \mathcal{K} ;
- for every path $\gamma : [0, 1] \rightarrow \mathcal{A}$ with $\gamma(0)$ and $\gamma(1)$ belonging to different components of \mathcal{A}^- , there exists a sub-path $\sigma := \gamma|_{[t', t'']} : [0, 1] \supseteq [t', t''] \rightarrow \mathcal{K}$, such that $\psi(\sigma(t)) \in \mathcal{B}$, $\forall t \in [t', t'']$, and, moreover, $\psi(\sigma(t'))$ and $\psi(\sigma(t''))$ belong to different components of \mathcal{B}^- .

A brief description of the relationship between the SAP relation and other “covering relations” in the literature on [expansive–contractive](#) maps can be found at the end of the present section.

A first crucial feature of the SAP relation is that, when it is satisfied with $\tilde{\mathcal{A}} = \tilde{\mathcal{B}}$,³ it ensures the existence of a fixed point localized in the compact set \mathcal{K} . In fact the following result does hold true.

Theorem 2.1. *Let $\tilde{\mathcal{P}} := (\mathcal{P}, \mathcal{P}^-)$ be an oriented parallelepiped of a metric space X and let $\psi : \mathcal{P} \rightarrow X$ be a function. If $\mathcal{K} \subseteq \mathcal{P}$ is a compact set such that*

$$(\mathcal{K}, \psi) : \tilde{\mathcal{P}} \rightleftarrows \tilde{\mathcal{P}},$$

then there exists at least a point $z \in \mathcal{K}$ with $\psi(z) = z$.

For a proof, see [\[33, pp. 307–308\]](#). Notice that the arguments employed therein are different from the ones used to prove the same result in the planar context (see, for instance, [\[18, pp. 3301–3302\]](#)), which are in fact much more elementary.

A graphical illustration of [Theorem 2.1](#) can be found in [Fig. 1](#), where it looks evident that, differently from the classical Rothe and Brouwer Theorems, we do not require that $\psi(\partial\mathcal{A}) \subseteq \mathcal{A}$ (or $\psi(\mathcal{A}) \subseteq \mathcal{A}$).

The most interesting case in view of detecting chaotic dynamics is when there exist pairwise disjoint compact sets playing the role of \mathcal{K} in [Definition 2.1](#). Indeed, applying [Theorem 2.1](#) with respect to each of them, we get a multiplicity of fixed points localized in those compact sets. Another crucial property of the SAP relation is that it is preserved under composition of maps, and thus, when dealing with the iterates of the function under consideration, it allows to detect the presence of periodic points of any period (for the precise statements, see Lemma A.1, Theorems A.1 and A.2 in [\[18\]](#), which can be directly transposed to the three-dimensional setting, with the same proofs).

³Note that this means both that \mathcal{A} and \mathcal{B} coincide as subsets of X and that they have the same orientation. In fact, it is easy to find counterexamples to [Theorem 2.1](#) if the latter property is violated (see, for instance, [\[36, p. 11\]](#)).

We now describe in [Definition 2.2](#) what we mean when we talk about “chaos” and we explain in [Theorem 2.2](#) which is the relationship between [Definition 2.2](#) and some well known concepts in the chaos literature. The proof of [Theorem 2.2](#) follows by the same arguments in [[18](#), Theorem 2.2]. Finally, we describe in [Theorem 2.3](#) which is the connection between [Definition 2.2](#) and the stretching relation in [Definition 2.1](#). We stress that [Theorem 2.3](#) is the main theoretical result we are going to apply in [Section 3](#) and that it can be shown exploiting the two properties of the SAP relation mentioned above. In fact, its proof follows by the same arguments in [[18](#), Theorem 2.3].

Definition 2.2. Let X be a metric space and let $\psi : X \supseteq D \rightarrow X$ be a function. Let also $m \geq 2$ be an integer. We say that ψ induces chaotic dynamics on m symbols on the set \mathcal{D} if there exist m nonempty pairwise disjoint compact subsets $\mathcal{K}_0, \dots, \mathcal{K}_{m-1}$ of \mathcal{D} such that, for each two-sided sequence on m symbols $(s_i)_{i \in \mathbb{Z}} \in \{0, \dots, m-1\}^{\mathbb{Z}}$, there exists a corresponding sequence $(w_i)_{i \in \mathbb{Z}} \in \mathcal{D}^{\mathbb{Z}}$ such that

$$w_i \in \mathcal{K}_{s_i} \text{ and } w_{i+1} = \psi(w_i), \quad \forall i \in \mathbb{Z}, \quad (2.1)$$

and, whenever $(s_i)_{i \in \mathbb{Z}}$ is a k -periodic sequence (that is, $s_{i+k} = s_i, \forall i \in \mathbb{Z}$) for some $k \geq 1$, there exists a k -periodic sequence $(w_i)_{i \in \mathbb{Z}} \in \mathcal{D}^{\mathbb{Z}}$ satisfying (2.1). To put the emphasis on the sets \mathcal{K}_j 's, we will also say that ψ induces chaotic dynamics on m symbols on the set \mathcal{D} relatively to $\mathcal{K}_0, \dots, \mathcal{K}_{m-1}$.

The above definition of chaos is similar to the one of chaos in the coin-tossing sense in [[37](#)]. The main difference between the two definitions concerns the fact that in [Definition 2.2](#) we have in addition the final requirement that the periodic sequences of symbols get realized by periodic ψ -orbits. We refer the interested reader to [[18](#)] for a more detailed discussion on the topic.

Let us now see in [Theorem 2.2](#) which are the main consequences of [Definition 2.2](#).

Theorem 2.2. Let ψ be a map that induces chaotic dynamics on m symbols on a set \mathcal{D} relatively to $\mathcal{K}_0, \dots, \mathcal{K}_{m-1}$ and that is continuous on

$$\mathcal{K} := \bigcup_{i=0}^{m-1} \mathcal{K}_i \subseteq \mathcal{D},$$

where $\mathcal{K}_0, \dots, \mathcal{K}_{m-1}$ and \mathcal{D} are like in [Definition 2.2](#). Introducing the nonempty compact set

$$\mathcal{I}_{\infty} := \bigcap_{n=0}^{\infty} \psi^{-n}(\mathcal{K}),$$

then there exists a nonempty compact set

$$\mathcal{I} \subseteq \mathcal{I}_{\infty} \subseteq \mathcal{K},$$

on which the following are fulfilled:

- (i) $\psi(\mathcal{I}) = \mathcal{I}$;
- (ii) $\psi|_{\mathcal{I}}$ is semi-conjugate to the Bernoulli shift on m symbols, that is, there exists a continuous map $\pi : \mathcal{I} \rightarrow \Sigma_m^+$, where $\Sigma_m^+ := \{0, \dots, m-1\}^{\mathbb{N}}$ is endowed with the distance

$$\hat{d}(\mathbf{s}', \mathbf{s}'') := \sum_{i \in \mathbb{N}} \frac{d(s'_i, s''_i)}{m^{i+1}}, \quad \text{for } \mathbf{s}' = (s'_i)_{i \in \mathbb{N}}, \mathbf{s}'' = (s''_i)_{i \in \mathbb{N}} \in \Sigma_m^+$$

($d(\cdot, \cdot)$ is the discrete distance on $\{0, \dots, m-1\}$, i.e., $d(s'_i, s''_i) = 0$ for $s'_i = s''_i$ and $d(s'_i, s''_i) = 1$ for $s'_i \neq s''_i$), such that the diagram

$$\begin{array}{ccc} \mathcal{I} & \xrightarrow{\psi} & \mathcal{I} \\ \pi \downarrow & & \downarrow \pi \\ \Sigma_m^+ & \xrightarrow{\sigma} & \Sigma_m^+ \end{array}$$

commutes, where $\sigma : \Sigma_m^+ \rightarrow \Sigma_m^+$ is the Bernoulli shift defined by $\sigma((s_i)_i) := (s_{i+1})_i, \forall i \in \mathbb{N}$;

(iii) the set of the periodic points of $\psi|_{\mathcal{I}_\infty}$ is dense in \mathcal{I} and the pre-image $\pi^{-1}(\mathbf{s}) \subseteq \mathcal{I}$ of every k -periodic sequence $\mathbf{s} = (s_i)_{i \in \mathbb{N}} \in \Sigma_m^+$ contains at least one k -periodic point.

Remark 2.1. According to [18, Theorem 2.2], from (ii) in Theorem 2.2 it follows that:

- $h_{\text{top}}(\psi) \geq h_{\text{top}}(\psi|_{\mathcal{I}}) \geq h_{\text{top}}(\sigma) = \log(m)$, where h_{top} is the topological entropy;
- there exists a compact invariant set $A \subseteq \mathcal{I}$ such that $\psi|_A$ is semi-conjugate to the Bernoulli shift on m symbols, topologically transitive and displays sensitive dependence on initial conditions.

As previously mentioned, in Theorem 2.3 we explain which is the relationship between Definitions 2.1 and 2.2.

Theorem 2.3. Let $\tilde{\mathcal{P}} := (\mathcal{P}, \mathcal{P}^-)$ be an oriented parallelepiped of a metric space X and let $\psi : \mathcal{P} \rightarrow X$ be a function. If $\mathcal{K}_0, \dots, \mathcal{K}_{m-1}$ are $m \geq 2$ pairwise disjoint compact subsets of \mathcal{P} such that

$$(\mathcal{K}_i, \psi) : \tilde{\mathcal{P}} \xrightarrow{\cong} \tilde{\mathcal{P}}, \quad \text{for } i = 0, \dots, m-1, \quad (2.2)$$

then ψ induces chaotic dynamics on m symbols on \mathcal{P} relatively to $\mathcal{K}_0, \dots, \mathcal{K}_{m-1}$.

Notice that if the function ψ in the above statement is also one-to-one on $\mathcal{K} := \bigcup_{i=0}^{m-1} \mathcal{K}_i$, then it is additionally possible to prove that ψ restricted to a suitable invariant subset of \mathcal{K} is semi-conjugate to the two-sided Bernoulli shift on m symbols $\sigma : \Sigma_m \rightarrow \Sigma_m$, $\sigma((s_i)_i) := (s_{i+1})_i, \forall i \in \mathbb{Z}$, where $\Sigma_m := \{0, \dots, m-1\}^{\mathbb{Z}}$ (see [23, Lemma 3.2]).⁴

We are now in position to explain what the SAP method consists in. Given a dynamical system generated by a map ψ , our technique consists in finding a subset \mathcal{P} of the domain of ψ homeomorphic to the unit cube and at least two disjoint compact subsets of \mathcal{P} for which the stretching property in (2.2) is satisfied (when \mathcal{P} is suitably oriented). In this way, Theorem 2.3 ensures the existence of chaotic dynamics in the sense of Definition 2.2 for the system under consideration. In particular, Theorem 2.2 then guarantees the positivity of the topological entropy for ψ , fact which is generally considered as one of the trademark features of chaos.

Notice that the number of compact sets for which the SAP property is satisfied coincides with the number of symbols in the conjugate Bernoulli shift, as well as with the number of crossings between \mathcal{P} and its ψ -image. The description of the stretching relation in Definition 2.1 using paths is indeed a mathematical formulation of the expansive–contractive behavior typical of the maps presenting topological horseshoes. The main difference with respect to other approaches in the related literature (see, for instance, [24–26]) is that the SAP method focuses, instead that on the image of generic sets, on how paths are transformed, and the compact sets \mathcal{K}_i 's play a crucial role in view of localizing fixed points and chaotic dynamics. The paper with the approach bearing more resemblances to the SAP method is [25], where connections and

⁴This is not the case in our application in Section 3. Indeed, as it looks clear from Fig. 2, the map F in (3.2) is not injective on the set $\mathcal{K}_0 \cup \mathcal{K}_1$ introduced in Theorem 3.1.

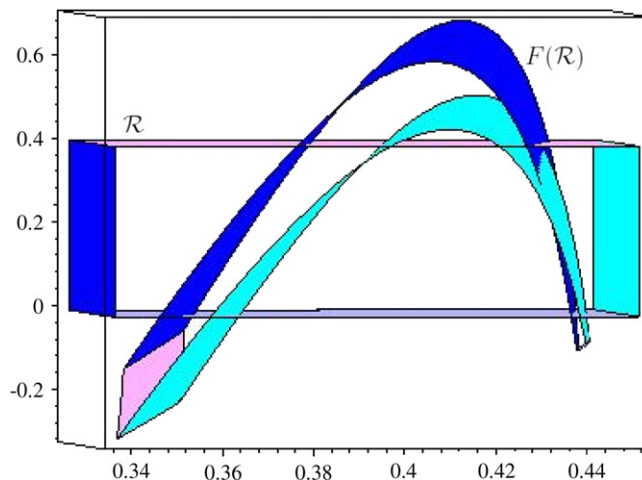


Fig. 2. A possible choice of the parallelepiped \mathcal{R} for system (3.1), according to conditions (H1)–(H5). It has been oriented by taking as $[\cdot]^-$ -set the union of the two horizontal faces \mathcal{R}_ℓ^- and \mathcal{R}_r^- defined in (3.4). In addition to $F(\mathcal{R}_\ell^-)$ and $F(\mathcal{R}_r^-)$, we also represent the image set of two vertical faces of \mathcal{R} . Notice that we used the same color to depict a set and its F -image set. (For interpretation of the references to colour in this figure legend, the reader is referred to the web version of this article.)

pre-connections play the role of our paths and sub-paths. However, the technique in [25], also due to the generality of the spaces considered, does not guarantee the existence of fixed points and periodic points, as shown in [25, Example 10].

3. The triopoly game model

In this section we apply the SAP method to an economic model belonging to the class of triopoly games, taken from [6].

By oligopoly, economists denote a market form characterized by the presence of a small number of firms. Triopoly is a special case of oligopoly where the firms are three. The term game refers to the fact that the players – in our case the firms – make their decisions reacting to each other actual or expected moves, following a suitable strategy. In particular, we will deal with a dynamic game where moves are repeated in time, at discrete, uniform intervals.

More precisely, the model analyzed can be described as follows.

The economy consists of three firms producing an identical commodity at a constant unit cost, not necessarily equal for the three firms. The commodity is sold in a single market at a price which depends on total output through a given inverse demand function, known to one firm (say, Firm 2) globally and to another firm (say, Firm 1) locally. In fact, Firm 1 linearly approximates the demand function around the latest realized pair of quantity and market price. Finally, Firm 3 does not know anything about the demand function and adopts a myopic adjustment mechanism, i.e., it increases or decreases its output according to the sign of the marginal profit from the last period. The goal of each firm is the maximization of profits, i.e., the difference between revenue and costs. The problem of each firm is to decide at the beginning of every time period t how much to produce in the same period on the basis of the limited information available and, in particular, on the expectations about its competitors' future decisions.

In what follows, we introduce the needed notation and the postulated assumptions:

1. Notation

x_t : output of Firm 1 at time t ;

y_t : output of Firm 2 at time t ;

z_t : output of Firm 3 at time t ;

p : unit price of the single commodity.

2. Inverse demand function

$$p := \frac{1}{x + y + z}.$$

3. Technology

The unit cost of production for firm i is equal to c_i , $i = 1, 2, 3$, where c_1, c_2, c_3 are (possibly different) positive constants.

4. Price approximation

Firm 1 observes the current market price p_t and the corresponding total supplied quantity $Q_t = x_t + y_t + z_t$. By using market experiments, that player obtains the slope of the demand function at the point (Q_t, p_t) and, in the absence of other information, it conjectures that the demand function, which has to pass through that point, is linear.

5. Expectations

In the presence of incomplete information concerning their competitors' future decisions (and therefore about future prices), Firms 1 and 2 are assumed to use naive expectations. This means that at each time t both Firms 1 and 2 expect that the other two firms will keep output unchanged w.r.t. the previous period. As shown in [6], the assumptions above lead to the following system of three difference equations in the variables x , y and z :

$$\begin{cases} x_{t+1} = \frac{2x_t + y_t + z_t - c_1(x_t + y_t + z_t)^2}{2} \\ y_{t+1} = \sqrt{\frac{x_t + z_t}{c_2}} - x_t - z_t \\ z_{t+1} = z_t + \alpha z_t \left(-c_3 + \frac{x_t + y_t}{(x_t + y_t + z_t)^2} \right) \end{cases} \quad (3.1)$$

where α is a positive parameter denoting the speed of Firm 3's adjustment to changes in profit and c_1, c_2, c_3 are the marginal costs.

We refer the interested reader to [6] for a more detailed explanation of the model, as well as for the derivation of (3.1).

As mentioned in the Introduction, in [6] Naimzada and Tramontana discuss the equilibrium solution of system (3.1) along with its stability and provide numerical evidence of the presence of chaotic dynamics. In particular, it is shown the existence of a double route to chaos: according to the parameter values, the Nash equilibrium can undergo a flip bifurcation or a Neimark–Sacker bifurcation. Moreover, in [6] the authors numerically find multistability of different coexisting attractors and identify their basins of attraction through a global analysis.

Hereinafter we will integrate that study rigorously proving that, for certain parameter configurations, system (3.1) exhibits chaotic behavior in the precise sense discussed in Section 2.⁵

⁵ Notice that, as we shall stress in Section 4, we only prove *existence* of an invariant, chaotic set, not its *attractiveness*.

In order to apply the SAP method to analyze system (3.1), it is expedient to represent it in the form of a continuous map $F = (F_1, F_2, F_3) : \mathbb{R}_+^3 \rightarrow \mathbb{R}^3$, with components

$$\begin{aligned} F_1(x, y, z) &:= \frac{2x + y + z - c_1(x + y + z)^2}{2}, \\ F_2(x, y, z) &:= \sqrt{\frac{x + z}{c_2}} - x - z, \\ F_3(x, y, z) &:= z + \alpha z \left(-c_3 + \frac{x + y}{(x + y + z)^2} \right). \end{aligned} \quad (3.2)$$

We prove that the SAP property for the map F is satisfied when choosing a generalized rectangle in the family of parallelepipeds of the first quadrant described analytically by

$$\mathcal{R} = \mathcal{R}(x_i, y_i, z_i) := \{(x, y, z) \in \mathbb{R}^3 : x_\ell \leq x \leq x_r, y_\ell \leq y \leq y_r, z_\ell \leq z \leq z_r\}, \quad (3.3)$$

with $x_\ell < x_r, y_\ell < y_r, z_\ell < z_r$ and $x_i, y_i, z_i, i \in \{\ell, r\}$, satisfying the conditions in Theorem 3.1.

The parallelepiped \mathcal{R} can be oriented by setting

$$\mathcal{R}_\ell^- := [x_\ell, x_r] \times [y_\ell, y_r] \times \{z_\ell\} \quad \text{and} \quad \mathcal{R}_r^- := [x_\ell, x_r] \times [y_\ell, y_r] \times \{z_r\}. \quad (3.4)$$

Consistently with [6], we choose the marginal costs as $c_1 = 0.4, c_2 = 0.55$ and $c_3 = 0.6$. On the other hand, in order to easily apply the SAP method we need the parameter α to be close to 17, while in [6] the presence of chaos is numerically proven for α around 8.⁶ The implications of this discrepancy will be discussed in Section 4.

Our result on system (3.1) can be stated as follows:

Theorem 3.1. *If the parameters of the map F defined in (3.2) assume the following values*

$$c_1 = 0.4, \quad c_2 = 0.55, \quad c_3 = 0.6, \quad \alpha = 17, \quad (3.5)$$

then, for any parallelepiped $\mathcal{R} = \mathcal{R}(x_i, y_i, z_i)$ belonging to the family described in (3.3), with $x_i, y_i, z_i, i \in \{\ell, r\}$, satisfying the conditions:

$$(H1) \quad z_\ell = 0;$$

$$(H2) \quad x_\ell + y_\ell > z_r \geq \sqrt{\frac{\alpha}{\alpha c_3 - 1}}(x_\ell + y_\ell) - (x_\ell + y_\ell) > 0;$$

$$(H3) \quad 2 \left(\sqrt{\frac{\alpha}{\alpha c_3 + 1}}(x_r + y_r) - (x_r + y_r) \right) > z_r;$$

$$(H4) \quad \frac{1}{c_1} - x_r > y_r + z_r > \frac{1}{2c_1} - x_\ell > 0, \quad \frac{1}{2c_1} - x_r > y_\ell + z_\ell, \quad x_r \geq \frac{1}{4c_1},$$

$$\frac{1}{2c_1} (1 - c_1(y_\ell + y_r + z_\ell + z_r)) \geq x_\ell > 0, \quad \sqrt{\frac{y_\ell + z_\ell}{c_1}} - (y_\ell + z_\ell) \geq x_\ell;$$

$$(H5) \quad x_\ell + z_\ell > \frac{1}{4c_2}, \quad y_r \geq \sqrt{\frac{x_\ell + z_\ell}{c_2}} - (x_\ell + z_\ell) > 0, \quad \sqrt{\frac{x_r + z_r}{c_2}} - (x_r + z_r) \geq y_\ell > 0,$$

and oriented as in (3.4), there exist two disjoint compact subsets $\mathcal{K}_0 = \mathcal{K}_0(\mathcal{R})$ and $\mathcal{K}_1 = \mathcal{K}_1(\mathcal{R})$ of \mathcal{R} such that

$$(\mathcal{K}_i, F) : \tilde{\mathcal{R}} \rightleftarrows \tilde{\mathcal{R}}, \quad \text{for } i = 0, 1. \quad (3.6)$$

⁶ As explained below, it would be possible to apply our technique with a lower value for α , at the cost of changing the parameter conditions in Theorem 3.1 and of making the computations in the proof much more complicated. However, it seems not possible to apply the SAP method to the first iterate of F when α is close to 8, which is the largest value considered in [6].

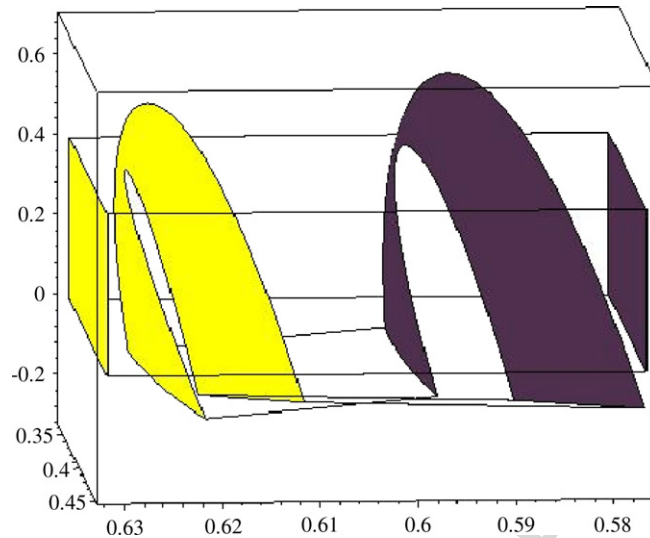


Fig. 3. This picture complements the previous one, by showing how the two vertical faces of \mathcal{R} not considered in Fig. 2 are transformed by the map F . Notice that we changed orientation with respect to Fig. 2, in order to better show the shape of the image sets. Again, the same color is used to depict a set and its F -image set. (For interpretation of the references to colour in this figure legend, the reader is referred to the web version of this article.)

Hence, the map F induces chaotic dynamics on two symbols on \mathcal{R} relatively to \mathcal{K}_0 and \mathcal{K}_1 and displays all the properties listed in Theorem 2.3.

Before proving Theorem 3.1, we make some comments on the conditions in (H1)–(H5). First of all, notice that those conditions imply that $x_\ell + z_\ell > 0$ and $x_\ell + y_\ell + z_\ell > 0$ and thus there are no issues with the definition of F on \mathcal{R} .⁷ We also remark that we chose to split (H1)–(H5) according to the corresponding conditions (C1)–(C5) in the next proof they allow to verify. Moreover we stress that the assumptions in (H1)–(H5) are consistent, i.e., there exist parameter configurations satisfying them all. For instance, we checked that they are fulfilled for $c_1 = 0.4$, $c_2 = 0.55$, $c_3 = 0.6$, $\alpha = 17$, $x_\ell = 0.5766666668$, $x_r = 0.6316666668$, $y_\ell = 0.3366666668$, $y_r = 0.4516666668$, $z_\ell = 0$, $z_r = 0.3951779684$. These are the same parameter values we used to draw Figs. 2–6, with the only exception of z_ℓ that in those pictures is slightly negative. Although this makes no sense from an economic viewpoint, as the variables x , y and z represent the output of the three firms, we made such choice in order to make the pictures easier to read. In fact, choosing $z_\ell = 0$, then $F(\mathcal{R}_\ell^-) \subseteq \mathcal{R}_\ell^-$ and thus the crucial set $F(\mathcal{R}_\ell^-)$ would have been not visible in Figs. 2–4. With this respect, we also remark that in Fig. 3 the x -axis has been reversed in order to make the double folding of $F(\mathcal{R})$ more evident.

In regard to the choice of the parameter values in (3.5), as mentioned above, they are the same as in [6], except for α , which is larger here. In fact, numerical exercises we performed show that when α increases it becomes easier to find a domain where to apply the SAP technique. On the other hand, it seems not possible to apply our method for a sensibly smaller value of α . The impossibility of reducing α much below 17 comes from the fact that, as it is immediate to verify, when such parameter decreases it becomes more and more difficult to have all conditions in (H2) and (H3) fulfilled and with $\alpha = 10$ it seems just impossible. The situation would slightly improve dealing with (C2) and (C3) below, instead of (C2) and (C3') as we actually do in order to simplify our argument, but still computer plots suggest it is not possible to have both conditions satisfied when $\alpha = 8$, that is the largest value considered in [6].

⁷ Notice that, with our conditions on the parameters, it is immediate to check that also the functions we will introduce in the proof of Theorem 3.1 will be well defined, even when not explicitly remarked.

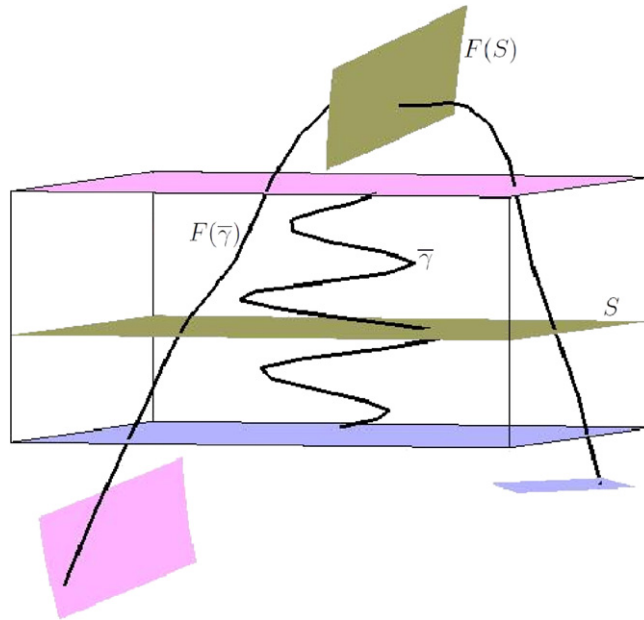


Fig. 4. With reference to the parallelepiped \mathcal{R} in Figs. 2 and 3, reproduced here at a different scale, we show that the F -image set of an arbitrary path γ joining in \mathcal{R} the two components of the boundary set \mathcal{R}^- intersects \mathcal{R} twice. In particular, this is due to the fact that the horizontal faces \mathcal{R}_ℓ^- and \mathcal{R}_r^- are mapped by F below \mathcal{R}_ℓ^- , in conformity with conditions (C1) and (C2), and that the flat surface S of the middle points w.r.t. the z -coordinate in \mathcal{R} is mapped by F above \mathcal{R}_r^- , in agreement with condition (C3') in the proof of Theorem 3.1.

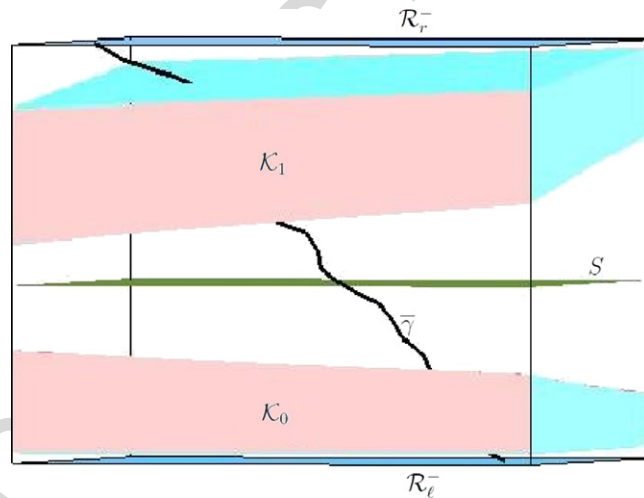


Fig. 5. Since $F(S) \cap \mathcal{R} = \emptyset$ (see Fig. 4), then $\mathcal{R} \cap F(\mathcal{R})$ is the union of two disjoint compact sets, we call \mathcal{K}_0 and \mathcal{K}_1 . In fact, as shown in the proof of Theorem 3.1, with such a choice it holds that $(\mathcal{K}_i, F) : \tilde{\mathcal{R}} \rightleftarrows \tilde{\mathcal{R}}$, for $i = 0, 1$.

Proof of Theorem 3.1. We show that, for the parameter values in (3.5), any choice of $x_i, y_i, z_i, i \in \{\ell, r\}$, fulfilling (H1)–(H5) guarantees that the image under the map F of any path $\gamma = (\gamma_1, \gamma_2, \gamma_3) : [0, 1] \rightarrow \mathcal{R} = \mathcal{R}(x_i, y_i, z_i)$ joining the sets \mathcal{R}_ℓ^- and \mathcal{R}_r^- defined in (3.4) satisfies the following conditions:

- 4 (C1) $F_3(\gamma(0)) \leq z_\ell$;
- 5 (C2) $F_3(\gamma(1)) \leq z_\ell$;

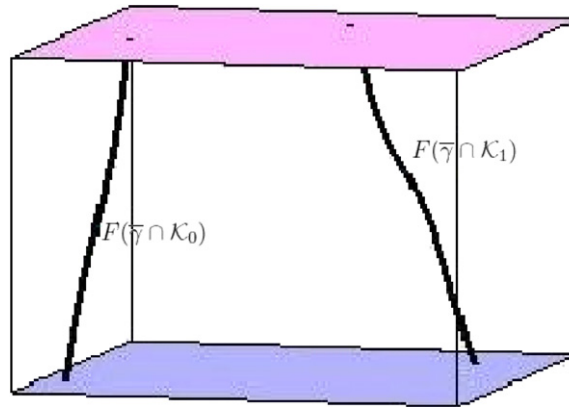


Fig. 6. Given the arbitrary path γ in Fig. 5 joining in \mathcal{R} the two components of \mathcal{R}^- , we show that the F -image sets of $\bar{\gamma} \cap \mathcal{K}_0$ and of $\bar{\gamma} \cap \mathcal{K}_1$ join \mathcal{R}_ℓ^- with \mathcal{R}_r^- , as required by the SAP property.

$$(C3) \exists t^* \in (0, 1) : F_3(\gamma(t^*)) > z_r;$$

$$(C4) F_1(\gamma(t)) \subseteq [x_\ell, x_r], \forall t \in [0, 1];$$

$$(C5) F_2(\gamma(t)) \subseteq [y_\ell, y_r], \forall t \in [0, 1].$$

Broadly speaking, conditions (C1)–(C3) describe an expansion with folding along the z -coordinate. In fact, the image $F \circ \gamma$ of any path γ joining in \mathcal{R} the sides \mathcal{R}_ℓ^- and \mathcal{R}_r^- crosses a first time the parallelepiped \mathcal{R} for $t \in (0, t^*)$ and then crosses \mathcal{R} back again for $t \in (t^*, 1)$. Conditions (C4) and (C5) imply instead a contraction along the x -coordinate and the y -coordinate, respectively.

Actually, in order to simplify the exposition, instead of the necessary condition (C3), we will check that the stronger and more specific requirement

$$(C3') F_3(x, y, \frac{z_\ell + z_r}{2}) > z_r, \forall (x, y) \in [x_\ell, x_r] \times [y_\ell, y_r],$$

is satisfied, which means that the inequality in (C3) holds for any $t^* \in (0, 1)$ such that $\gamma(t^*) = (x, y, \frac{x_\ell + x_r}{2})$, for some $(x, y) \in [x_\ell, x_r] \times [y_\ell, y_r]$. Notice that

$$S := \left\{ \left(x, y, \frac{z_\ell + z_r}{2} \right) : (x, y) \in [x_\ell, x_r] \times [y_\ell, y_r] \right\} \subseteq \mathcal{R} \quad (3.7)$$

is the flat surface of middle points w.r.t. the z -coordinate in \mathcal{R} depicted in Fig. 4.

Setting

$$\mathcal{R}_0 := \left\{ (x, y, z) \in \mathbb{R}^3 : (x, y) \in [x_\ell, x_r] \times [y_\ell, y_r], z \in \left[z_\ell, \frac{z_\ell + z_r}{2} \right] \right\},$$

$$\mathcal{R}_1 := \left\{ (x, y, z) \in \mathbb{R}^3 : (x, y) \in [x_\ell, x_r] \times [y_\ell, y_r], z \in \left[\frac{z_\ell + z_r}{2}, z_r \right] \right\},$$

and

$$\mathcal{K}_0 := \mathcal{R}_0 \cap F(\mathcal{R}) \quad \text{and} \quad \mathcal{K}_1 := \mathcal{R}_1 \cap F(\mathcal{R})$$

(see Fig. 5), we claim that (C1), (C2), (C3'), (C4) and (C5) together imply (3.6). Notice at first that \mathcal{K}_0 and \mathcal{K}_1 are disjoint because, thanks to condition (C3'), the set S in (3.7) is mapped by F outside \mathcal{R} (see Fig. 4), and that F is continuous on $\mathcal{K}_0 \cup \mathcal{K}_1$, because it is continuous on \mathcal{R} . Furthermore, by (C1), (C2)

and (C3'), for every path $\gamma : [0, 1] \rightarrow \mathcal{R}$ such that $\gamma(0)$ and $\gamma(1)$ belong to different components of \mathcal{R}^- , there exist two disjoint sub-intervals $[t'_0, t''_0], [t'_1, t''_1] \subseteq [0, 1]$ such that, setting $\sigma_0 := \gamma|_{[t'_0, t''_0]} : [t'_0, t''_0] \rightarrow \mathcal{K}_0$ and $\sigma_1 := \gamma|_{[t'_1, t''_1]} : [t'_1, t''_1] \rightarrow \mathcal{K}_1$, it holds that $F(\sigma_0(t'_0))$ and $F(\sigma_0(t''_0))$ belong to different components of \mathcal{R}^- , as well as $F(\sigma_1(t'_1))$ and $F(\sigma_1(t''_1))$. Moreover, from (C4) and (C5) it follows that $F(\sigma_0(t)) \in \mathcal{R}, \forall t \in [t'_0, t''_0]$ and $F(\sigma_1(t)) \in \mathcal{R}, \forall t \in [t'_1, t''_1]$.

This means that $(\mathcal{K}_i, F) : \tilde{\mathcal{R}} \rightleftarrows \tilde{\mathcal{R}}, i = 0, 1$, and our claim is thus proved.

Once that the stretching condition in (3.6) is achieved, the conclusion of the theorem follows by Theorem 2.3.⁸

In order to complete the proof, let us verify that any choice of the parameters as in (3.5) and of the domain $\mathcal{R} = \mathcal{R}(x_i, y_i, z_i)$ in agreement with (H1)–(H5) implies that conditions (C1), (C2), (C3'), (C4) and (C5) are fulfilled for any path $\gamma : [0, 1] \rightarrow \mathcal{R}$ joining \mathcal{R}_ℓ^- and \mathcal{R}_r^- .⁹ In so doing, we will prove that the inequality in (C1) is indeed an equality.

Let us start with the verification of (C1). Since $F_3(x, y, z) = z \left(1 - \alpha c_3 + \frac{\alpha(x+y)}{(x+y+z)^2} \right)$ and $\gamma(0) \in \mathcal{R}_\ell^- = [x_\ell, x_r] \times [y_\ell, y_r] \times \{z_\ell\} = [x_\ell, x_r] \times [y_\ell, y_r] \times \{0\}$ by (H1), it then follows that $\gamma_3(0) = 0$ and thus $0 = F_3(\gamma(0)) \leq z_\ell = 0$, as desired.

In regard to (C2), we have to verify that $F_3|_{\mathcal{R}_r^-} \leq 0$, that is, $F_3(x, y, z_r) \leq 0, \forall (x, y) \in [x_\ell, x_r] \times [y_\ell, y_r]$. Setting $A := x + y$, we consider, instead of $F_3|_{\mathcal{R}_r^-}$, the one-dimensional function¹⁰

$$\phi : [x_\ell + y_\ell, x_r + y_r] \rightarrow \mathbb{R}, \quad \phi(A) := z_r \left(1 - \alpha c_3 + \frac{\alpha A}{(A + z_r)^2} \right).$$

Computing the first derivative of ϕ , we get $\phi'(A) = z_r \alpha \left(\frac{-A + z_r}{(A + z_r)^3} \right)$, which vanishes at $A = z_r$. However, since by (H2) we have $x_\ell + y_\ell > z_r$, then $\phi'(A) < 0, \forall A \in [x_\ell + y_\ell, x_r + y_r]$. Hence, $F_3|_{\mathcal{R}_r^-} \leq F_3(x_\ell, y_\ell, z_r)$ and thus, in order to have (C2) satisfied, it suffices that $F_3(x_\ell, y_\ell, z_r) \leq 0$. Imposing such condition, we find $z_r \left(1 - \alpha c_3 + \frac{\alpha(x_\ell + y_\ell)}{(x_\ell + y_\ell + z_r)^2} \right) \leq 0$, which is fulfilled when $\frac{\alpha c_3 - 1}{\alpha} \geq \frac{x_\ell + y_\ell}{(x_\ell + y_\ell + z_r)^2}$. Making z_r explicit, this holds when $z_r \geq \sqrt{\frac{\alpha}{\alpha c_3 - 1}(x_\ell + y_\ell)} - (x_\ell + y_\ell)$, that is, when (H2) is fulfilled. Notice that the latter is a “true” restriction, since, still by (H2), the right hand side of the above inequality is positive. The verification of (C2) is complete.

As regards (C3'), we need to check that $F_3(x, y, \frac{z_\ell + z_r}{2}) > z_r, \forall (x, y) \in [x_\ell, x_r] \times [y_\ell, y_r]$, that is, recalling the definition of S in (3.7), $F_3|_S > z_r$. Notice that, by (H1), $\frac{z_\ell + z_r}{2} = \frac{z_r}{2}$. Analogously to what done above, instead of $F_3|_S$, let us consider the one-dimensional function

$$\varphi : [x_\ell + y_\ell, x_r + y_r] \rightarrow \mathbb{R}, \quad \varphi(A) := \frac{z_r}{2} \left(1 - \alpha c_3 + \frac{\alpha A}{(A + \frac{z_r}{2})^2} \right).$$

Since $x_\ell + y_\ell > z_r > \frac{z_r}{2}$, by the previous analysis we know that $\varphi(A) \geq \varphi(x_r + y_r) = F_3(x_r, y_r, \frac{z_r}{2})$. Hence, in order to have $F_3|_S > z_r$, it suffices that $F_3(x_r, y_r, \frac{z_r}{2}) > z_r$, that is,

$$\frac{z_r}{2} \left(1 - \alpha c_3 + \frac{\alpha(x_r + y_r)}{(x_r + y_r + \frac{z_r}{2})^2} \right) > z_r.$$

⁸ Notice that, by the choice of \mathcal{K}_0 and \mathcal{K}_1 , the invariant chaotic set $\mathcal{I} \subseteq \mathcal{K}_0 \cup \mathcal{K}_1$ in Definition 2.2 lies entirely in the first quadrant and therefore makes economic sense for the application in question.

⁹ Just to fix the ideas, in what follows we will assume that $\gamma(0) \in \mathcal{R}_\ell^-$ and $\gamma(1) \in \mathcal{R}_r^-$.

¹⁰ In several steps of the proof, instead of studying the original problem, through a substitution we will be lead to consider a lower-dimensional one. Alternatively, we could use the Kuhn–Tucker Theorem for constrained maximization problems. We decided to follow the former approach because it is more elementary and requires less computations. However, we stress that the two approaches require to impose the same conditions (H1)–(H5) on the parameters.

Since $z_r > 0$, making z_r explicit, we find

$$z_r < 2 \left(\sqrt{\frac{\alpha}{\alpha c_3 + 1} (x_r + y_r)} - (x_r + y_r) \right)$$

and this condition is satisfied thanks to (H3). Hence (C3) is verified.

In order to check (C4), we need to show the two inequalities $F_1(x, y, z) \leq x_r$, $\forall (x, y, z) \in \mathcal{R}$ and $F_1(x, y, z) \geq x_\ell$, $\forall (x, y, z) \in \mathcal{R}$, which are satisfied if

$$\max_{(x,y,z) \in \mathcal{R}} F_1(x, y, z) \leq x_r \quad \text{and} \quad \min_{(x,y,z) \in \mathcal{R}} F_1(x, y, z) \geq x_\ell,$$

respectively.¹¹

Instead of considering $F_1|_{\mathcal{R}}$, setting $B := y + z$ and $T := [x_\ell, x_r] \times [y_\ell + z_\ell, y_r + z_r]$, we deal with the bi-dimensional function

$$\Phi : T \rightarrow \mathbb{R}, \quad \Phi(x, B) := \frac{2x + B - c_1(x + B)^2}{2},$$

whose partial derivatives are

$$\frac{\partial \Phi}{\partial x} = 1 - c_1(x + B) \quad \text{and} \quad \frac{\partial \Phi}{\partial B} = \frac{1}{2} - c_1(x + B).$$

Since they do not vanish contemporaneously, there are no critical points in the interior of T . We then study Φ on the boundary of its domain.

As concerns $\Phi_1(B) := \Phi|_{\{x_\ell\} \times [y_\ell + z_\ell, y_r + z_r]}(x, B) = \Phi(x_\ell, B)$, we have that $\Phi'_1(B) = \frac{1}{2} - c_1(x_\ell + B)$, which vanishes at $\bar{B} = \frac{1}{2c_1} - x_\ell$. This is the maximum point of Φ_1 if $\bar{B} \in [y_\ell + z_\ell, y_r + z_r]$. But that is guaranteed by the conditions in (H4).

Similarly, setting $\Phi_2(B) := \Phi|_{\{x_r\} \times [y_\ell + z_\ell, y_r + z_r]}(x, B) = \Phi(x_r, B)$, we find that its maximum point, still by (H4), is given by $\hat{B} = \frac{1}{2c_1} - x_r \in [y_\ell + z_\ell, y_r + z_r]$.

In regard to $\Phi_3(x) := \Phi|_{[x_\ell, x_r] \times \{y_\ell + z_\ell\}}(x, B) = \Phi(x, y_\ell + z_\ell)$, we have $\Phi'_3(x) = 1 - c_1(x + y_\ell + z_\ell)$, which vanishes at $\bar{x} = \frac{1}{c_1} - (y_\ell + z_\ell)$. By the conditions in (H4), $\bar{x} > x_r$ and thus $\Phi_3(x)$ is increasing on $[x_\ell, x_r]$. Analogously, since $\hat{x} = \frac{1}{c_1} - (y_r + z_r) > x_r$, it holds that $\Phi_4(x) := \Phi|_{[x_\ell, x_r] \times \{y_r + z_r\}}(x, B) = \Phi(x, y_r + z_r)$ is increasing on $[x_\ell, x_r]$. Summarizing, the two candidates for the maximum point of Φ on T are $(x_\ell, \frac{1}{2c_1} - x_\ell)$ and $(x_r, \frac{1}{2c_1} - x_r)$. A direct computation shows that $\Phi(x_\ell, \frac{1}{2c_1} - x_\ell) < \Phi(x_r, \frac{1}{2c_1} - x_r)$, and thus $\max_{(x,y,z) \in \mathcal{R}} F_1(x, y, z) = \Phi(x_r, \frac{1}{2c_1} - x_r)$. Hence, it is now easy to verify that the inequality $\max_{(x,y,z) \in \mathcal{R}} F_1(x, y, z) \leq x_r$ is satisfied when $x_r \geq \frac{1}{4c_1}$, the latter being among the assumptions in (H4).

The analysis above also suggests that the two candidates for the minimum point of Φ on T are $(x_\ell, y_\ell + z_\ell)$ and $(x_\ell, y_r + z_r)$. Straightforward calculations show that, if $x_\ell \leq \frac{1}{2c_1} (1 - c_1(y_\ell + y_r + z_\ell + z_r))$, then $\Phi(x_\ell, y_\ell + z_\ell) \leq \Phi(x_\ell, y_r + z_r)$. Hence, again by (H4), $\min_{(x,y,z) \in \mathcal{R}} F_1(x, y, z) = \Phi(x_\ell, y_\ell + z_\ell)$. The inequality $\min_{(x,y,z) \in \mathcal{R}} F_1(x, y, z) \geq x_\ell$ is thus satisfied when $\sqrt{\frac{y_\ell + z_\ell}{c_1}} - (y_\ell + z_\ell) \geq x_\ell$, which is among the conditions in (H4).

This concludes the verification of (C4).

Let us finally turn to (C5). In order to check it, we have to show that

$$\max_{(x,y,z) \in \mathcal{R}} F_2(x, y, z) \leq y_r \quad \text{and} \quad \min_{(x,y,z) \in \mathcal{R}} F_2(x, y, z) \geq y_\ell. \quad (3.8)$$

¹¹ Notice that such maximum and minimum values exist by the Weierstrass Theorem.

1 Instead of $F_2|_{\mathcal{R}}$, setting $D := x + z$, we deal with the one-dimensional function

$$2 \quad \psi : [x_\ell + z_\ell, x_r + z_r] \rightarrow \mathbb{R}, \quad \psi(D) := \sqrt{\frac{D}{c_2}} - D,$$

3 whose derivative is $\psi'(D) = \frac{1}{2\sqrt{c_2 D}} - 1$. It vanishes at $\bar{D} = \frac{1}{4c_2}$, which by (H5) is smaller than $x_\ell + z_\ell$. Thus
 4 $\max_{(x,y,z) \in \mathcal{R}} F_2(x, y, z) = \psi(x_\ell + z_\ell)$ and $\min_{(x,y,z) \in \mathcal{R}} F_2(x, y, z) = \psi(x_r + z_r)$. Hence, the first condition in
 5 (3.8) is satisfied if $\psi(x_\ell + z_\ell) \leq y_r$ and the second condition is fulfilled if $\psi(x_r + z_r) \geq y_\ell$. It is easy to see
 6 that both inequalities are fulfilled thanks to (H5) and this concludes the verification of (C5).

7 The proof is complete. \square

8 **Remark 3.1.** We stress that, slightly modifying the conditions for the construction of the parallelepiped
 9 \mathcal{R} in the statement of [Theorem 3.1](#), it is possible to obtain a robust result on the existence of chaotic
 10 dynamics, i.e., a result stable with respect to small changes in the value of the model parameters c_1, c_2, c_3
 11 and α in (3.5). To this aim, it suffices to replace the weak inequalities in (H2), (H4) and (H5) with strict
 12 inequalities (and, correspondingly, set strict inequalities and inclusions in (C2), (C4) and (C5)) and exploit
 13 the continuity of the map F . Notice that the parameter values in (3.5) satisfy even those stricter conditions.
 14 The only exception¹² in such procedure is given by (H1) (and, correspondingly, (C1)) that, in the specific
 15 example considered, cannot be written with strict inequalities. This is due to the fact that, since the variable
 16 z represents an output, we cannot take $z_\ell < 0$, while, as it is easy to verify, with $z_\ell > 0$ condition (C1) would
 17 not hold and the geometry required to apply the SAP method would be missing. On the other hand, $(x, y, 0)$
 18 is a fixed point for the map F_3 , for every $(x, y) \in \mathbb{R}_+^2$, and thus, under condition (H1), $F_3(\mathcal{R}_\ell^-) = 0 = z_\ell$,
 19 independently of the choice of the model parameters. This means that, even if it is not possible to modify
 20 condition (H1), the above suggested changes suffice to make [Theorem 3.1](#) stable with respect to small
 21 perturbations in the parameter values. However, in the particular context considered in the present section,
 22 it seems not possible to obtain a result stable with respect to more general perturbations on F , because
 23 our proof heavily relies on the expression of F_3 and its fixed points. For a precise formulation of a related
 24 perturbative result in the bi-dimensional setting, see [38, Corollary 2.1].

25 4. Conclusions

26 In this paper we have recalled what the SAP method consists in and we have applied that topological
 27 technique to rigorously prove the existence of robust chaotic sets for the triopoly game model in [6]. By
 28 “chaotic sets” we mean invariant domains on which the map describing the system under consideration is
 29 semiconjugate to the Bernoulli shift (implying the features in [Remark 2.1](#)) and where periodic points are
 30 dense. By “robustness” we mean that our result is stable with respect to small parameter perturbations.
 31 However, we stress that we did not say anything about the attractivity of those chaotic sets. In fact, in
 32 general, the SAP method does not allow to draw any conclusion in such direction. For instance, when
 33 performing numeric simulations for the parameter values in (3.5), no attractor appears on the computer
 34 screen. The same issue emerged with the bi-dimensional models considered in [18]. The fact that the chaotic
 35 set is repulsive can be a good signal as regards the overlapping generations model therein, for which we
 36 studied a backward moving system, since the forward moving one was defined only implicitly and it was
 37 not possible to invert it. Indeed, as argued in [18], a repulsive chaotic set for the backward moving system
 38 possibly gets transformed into an attractive one for a related forward moving system through Inverse Limit
 39 Theory (ILT). In general, however, one just deals with a forward moving dynamical system and this kind
 40 of argument cannot be employed. For instance, both in the duopoly game model in [18] and in the triopoly

¹² Condition (H3), and correspondingly (C3), do not need any intervention, as they are already written in the “stricter” form.

game model analyzed in the present paper, we are able to prove the presence of chaos for the same parameter values considered in the literature, except for a bit larger speed of adjustment α . It makes economic sense that complex dynamics arise when firms are more reactive, but unfortunately for such parameter values no chaotic attractors can be found via numerical simulations.

What we want to stress is that this is not a limit of the SAP method: such issue is instead related to the possibility of performing computations by hands. To see what is the point, let us consider the well-known case of the logistic map $f : [0, 1] \rightarrow \mathbb{R}$, $f(x) = \mu x(1 - x)$, with $\mu > 0$. As observed in [18], if we want to show the presence of chaos for it via the SAP method¹³ by looking at the first iterate, then we need $\mu > 4$. In this case, however, the interval $[0, 1]$ is not mapped into itself and for almost all initial points in $[0, 1]$ forward iterates limit to $-\infty$. If we consider instead the second iterate, the SAP method may be applied for values less than 4, for which chaotic attractors do exist. See [18] for further details.


This simple example aims to suggest that working with higher iterates may allow to reach an agreement between the conditions needed to employ the SAP method and those to find chaotic attractors via numerical simulations.

A possible direction of future study can then be the study of economically interesting but simple enough models, so that it is possible to deal with higher iterates, in the attempt of rigorously proving the presence of chaos via the SAP technique for parameter values for which also computer simulations indicate the same kind of behavior.


Still in regard to chaotic attractors, we have observed that the SAP method works well for models presenting Hénon-like attractors, due to the presence of a double folding, in turn related to the geometry required to apply our technique. On the other hand, a preliminary analysis seems to suggest that the SAP method is not easily applicable to models presenting a Neimark–Sacker bifurcation leading to chaos. A more detailed investigation of such kind of framework will be pursued, as well.

A further possible direction of future study is the analysis of continuous-time economic models with our technique, maybe in the context of LTMs, for systems switching between two different regimes, such as gross complements and gross substitutes.

Acknowledgments

Many thanks to Prof. Gardini,  Naimzada, Prof. Pini and Prof. Zanolin for useful discussions during the preparation of the paper.

References

- [1]  Agiza, On the analysis of stability, bifurcation, chaos and chaos control of Kopel map, *Chaos Solitons Fractals* 10 (9) 1909–1916.
- [2] I. Bischì, F. Tramontana, Three-dimensional discrete-time Lotka–Volterra models with an application to industrial clusters, *Commun. Nonlinear Sci. Numer. Simul.* 15 (2010) 3000–3014.
- [3] F. Tramontana, L. Gardini, R. Dieci, F. Westerhoff, Global bifurcations in a three-dimensional financial model of bull and bear interactions, in: *Nonlinear Dynamics in Economics, Finance and the Social Sciences*, Springer, Berlin, 2010, pp. 333–352.
- [4] S. Yousefi, Y. Maistrenko, S. Popovych, The complex dynamics in a simple model of interdependent open economies, *Discrete Dyn. Nat. Soc.* 5 (2000) 161–177.
- [5] J.S. Cánovas, Reducing competitors in Cournot–Puu oligopoly, *Nonlinear Anal. RWA* 13 (2012) 1772–1779.
- [6] A. Naimzada, F. Tramontana, Double route to chaos in an heterogeneous triopoly game, Working Paper. Available at: <http://ideas.repec.org/p/pav/wpaper/149.html>.

¹³ Notice that, in the one-dimensional framework, parallelepipeds become intervals and the $[\cdot]^-$ -sets are simply the end points of such intervals. Hence, in that context, the SAP relation produces only a stretching effect, without any compressive direction, and the induced behavior looks similar to that of turbulent functions and horseshoes for one-dimensional maps (see [39–42]). In this perspective, the SAP method may be seen as an higher-dimensional counterpart of those one-dimensional approaches.

- [7] E.M. Elabbasy, H.N. Agiza, A.A. Elsadany, Analysis of nonlinear triopoly game with heterogeneous players, *Comput. Math. Appl.* 57 (2009) 488–499.
- [8] T. Puu, Complex dynamics with three oligopolists, *Chaos Solitons Fractals* 7 (1996) 2075–2081.
- [9] F. Tramontana, A.A. Elsadany, Heterogeneous triopoly game with isoelastic demand function, *Nonlinear Dynam.* 68 (2012) 187–193.
- [10] H.N. Agiza, Explicit stability zones for Cournot games with 3 and 4 competitors, *Chaos Solitons Fractals* 9 (1998) 1955–1966.
- [11] A. Agliari, L. Gardini, T. Puu, The dynamics of a triopoly Cournot game, *Chaos Solitons Fractals* 11 (2000) 2531–2560.
- [12] H. Richter, A. Stolk, Control of the triple chaotic attractor in a Cournot triopoly model, *Chaos Solitons Fractals* 20 (2004) 409–413.
- [13] I. Bischi, L. Sbragia, F. Szidarovszky, Learning the demand function in a repeated Cournot oligopoly game, *Internat. J. Systems Sci.* 39 (2008) 403–419.
- [14] C. Chiarella, F. Szidarovszky, The nonlinear Cournot model under uncertainty with continuously distributed time lags, *Cent. Eur. J. Oper. Res.* 9 (2001) 183–196.
- [15] C. Chiarella, F. Szidarovszky, Dynamic oligopolies without full information and with continuously distributed time lags, *J. Econ. Behav. Organ.* 54 (2004) 495–511.
- [16] E.M. Elabbasy, H.N. Agiza, A.A. Elsadany, H. EL-Metwally, The dynamics of triopoly game with heterogeneous players, *Int. J. Nonlinear Sci.* 3 (2007) 83–90.
- [17] W. Ji, Chaos and control of game model based on heterogeneous expectations in electric power triopoly, *Discrete Dyn. Nat. Soc.* 2009 (2009) 8. Article ID 469564.
- [18] A. Medio, M. Pireddu, F. Zanolin, Chaotic dynamics for maps in one and two dimensions. A geometrical method and applications to economics, *Internat. J. Bifur. Chaos Appl. Sci. Engrg.* 19 (2009) 3283–3309.
- [19] R.W. Easton, Isolating blocks and symbolic dynamics, *J. Differential Equations* 17 (1975) 96–118.
- [20] K. Mischaikow, M. Mrozek, Isolating neighborhoods and chaos, *Japan J. Indust. Appl. Math.* 12 (1995) 205–236.
- [21] R. Szrednicki, K. Wójcik, A geometric method for detecting chaotic dynamics, *J. Differential Equations* 135 (1997) 66–82.
- [22] A. Pascoletti, M. Pireddu, F. Zanolin, Multiple periodic solutions and complex dynamics for second order ODEs via linked twist maps, *Electron. J. Qual. Theory Differ. Equ.* 14 (2008) 1–32. Proc. 8th Coll. Qualitative Theory of Diff. Equ.
- [23] M. Pireddu, F. Zanolin, Chaotic dynamics in the Volterra predator–prey model via linked twist maps, *Opuscula Math.* 28 (2008) 567–592.
- [24] K. Burns, H. Weiss, A geometric criterion for positive topological entropy, *Comm. Math. Phys.* 172 (1995) 95–118.
- [25] J. Kennedy, J.A. Yorke, Topological horseshoes, *Trans. Amer. Math. Soc.* 353 (2001) 2513–2530.
- [26] P. Zgliczyński, M. Gidea, Covering relations for multidimensional dynamical systems, *J. Differential Equations* 202 (2004) 32–58.
- [27] S. Smale, Diffeomorphism with many periodic points, in: *Differential and Combinatorial Topology (A Symposium in Honor of Marston Morse)*, Princeton Univ. Press, Princeton, NJ, 1965, pp. 63–80.
- [28] R. Burton, R.W. Easton, Ergodicity of linked twist maps, in: *Global Theory of Dynamical Systems (Proc. Internat. Conf., Northwestern Univ., Evanston, Ill., 1979)*, in: *Lecture Notes in Math.*, vol. 819, Springer, Berlin, 1980, pp. 35–49.
- [29] R.L. Devaney, Subshifts of finite type in linked twist mappings, *Proc. Amer. Math. Soc.* 71 (1978) 334–338.
- [30] F. Przytycki, Periodic points of linked twist mappings, *Studia Math.* 83 (1986) 1–18.
- [31] A. Ruiz-Herrera, F. Zanolin, A simple example of chaotic dynamics in 3D systems via stretching along paths, *Ann. Mat. Pura Appl.* (2012) <http://dx.doi.org/10.1007/s10231-012-0271-0>.
- [32] A. Ruiz-Herrera, F. Zanolin, Periodic solutions and chaotic dynamics in 3D equations with applications to Lotka–Volterra systems, Working Paper.
- [33] M. Pireddu, F. Zanolin, Cutting surfaces and applications to periodic points and chaotic-like dynamics, *Topol. Methods Nonlinear Anal.* 30 (2007) 271–320.
- [34] D. Papini, F. Zanolin, On the periodic boundary value problem and chaotic-like dynamics for nonlinear Hill’s equations, *Adv. Nonlinear Stud.* 4 (2004) 71–91.
- [35] D. Papini, F. Zanolin, Fixed points, periodic points, and coin-tossing sequences for mappings defined on two-dimensional cells, *Fixed Point Theory Appl.* 2004 (2004) 113–134.
- [36] M. Pireddu, Fixed points and chaotic dynamics for expansive-contractive maps in Euclidean spaces, with some applications. Ph.D. Thesis. Available at: [arXiv:0910.3832v1](http://arxiv.org/abs/0910.3832v1).
- [37] U. Kirchgraber, D. Stoffer, On the definition of chaos, *ZAMM Z. Angew. Math. Mech.* 69 (1989) 175–185.
- [38] A. Ruiz-Herrera, Chaos in predator–prey systems with/without impulsive effect, *Nonlinear Anal. RWA* 13 (2012) 977–986.
- [39] L.S. Block, W.A. Coppel, Stratification of continuous maps of an interval, *Trans. Amer. Math. Soc.* 297 (1986) 587–604.
- [40] L.S. Block, W.A. Coppel, Dynamics in One Dimension, in: *Lecture Notes in Mathematics*, vol. 1513, Springer-Verlag, Berlin, 1992.
- [41] A. Blokh, E. Teoh, How little is little enough? *Discrete Contin. Dyn. Syst.* 9 (2003) 969–978.
- [42] P. Glendinning, Stability, Instability and Chaos: An Introduction to the Theory of Nonlinear Differential Equations, in: *Cambridge Texts in Applied Mathematics*, Cambridge University Press, Cambridge, 1994.